Tectonic interpretation of the Andrew Bain transform fault: Southwest Indian Ocean

John G Sclater, Nancy R Grindlay, John A Madsen, Céline Rommevaux-Jestin

Geochemistry Geophysics Geosystems G3
AN ELECTRONIC JOURNAL OF THE EARTH SCIENCES
Published by AGU and the Geochemical Society

Article
Volume 6, Number 9
27 September 2005
Q09K10, doi:10.1029/2005GC000951
ISSN: 1525-2027

Tectonic interpretation of the Andrew Bain transform fault: Southwest Indian Ocean

John G. Sclater
Geosciences Research Division 0220, Scripps Institution of Oceanography, University of California San Diego, La Jolla, California 92093-0220, USA (jsclater@ucsd.edu)

Nancy R. Grindlay
Center for Marine Science, University of North Carolina, Wilmington, Wilmington, North Carolina 28409, USA (grindlayn@uncw.edu)

John A. Madsen
Department of Geology, University of Delaware, Newark, Delaware 19716, USA (jmadsen@udel.edu)

Celine Rommevaux-Jestin
Institut de Physique du Globe de Paris, CNRS-UPMC, 4 Place Jussieu, F-75252 Paris Cedex 05, France (rommevau@ipgp.jussieu.fr)

[1] Between 25°E and 35°E, a suite of four transform faults, Du Toit, Andrew Bain, Marion, and Prince Edward, offsets the Southwest Indian Ridge (SWIR) left laterally 1230 km. The Andrew Bain, the largest, has a length of 750 km and a maximum transform domain width of 120 km. We show that, currently, the Nubia/Somalia plate boundary intersects the SWIR east of the Prince Edward, placing the Andrew Bain on the Nubia/Antarctica plate boundary. However, the overall trend of its transform domain lies 10° clockwise of the predicted direction of motion for this boundary. We use four transform-parallel multibeam and magnetic anomaly profiles, together with relocated earthquakes and focal mechanism solutions, to characterize the morphology and tectonics of the Andrew Bain. Starting at the southwestern ridge-transform intersection, the relocated epicenters follow a 450-km-long, 20-km-wide, 6-km-deep western valley. They cross the transform domain within a series of deep overlapping basins bounded by steep inward dipping arcuate scarps. Eight strike-slip and three dip-slip focal mechanism solutions lie within these basins. The earthquakes can be traced to the northeastern ridge-transform intersection via a straight, 100-km-long, 10-km-wide, 4.5-km-deep eastern valley. A striking set of seismically inactive NE-SW trending en echelon ridges and valleys, lying to the south of the overlapping basins, dominates the eastern central section of the transform domain. We interpret the deep overlapping basins as two pull-apart features connected by a strike-slip basin that have created a relay zone similar to those observed on continental transforms. This transform relay zone connects three closely spaced overlapping transform faults in the southwest to a single transform fault in the northeast. The existence of the transform relay zone accounts for the difference between the observed and predicted trend of the Andrew Bain transform domain. We speculate that between 20 and 3.2 Ma, an oblique accretionary zone jumping successively northward created the en echelon ridges and valleys in the eastern central portion of the domain. The style of accretion changed to that of a transform relay zone, during a final northward jump, at 3.2 Ma.

Components: 11,632 words, 7 figures, 3 tables.

Keywords: megatransform; tectonics.

Index Terms: 3039 Marine Geology and Geophysics: Oceanic transform and fracture zone processes; 3040 Marine Geology and Geophysics: Plate tectonics (8150, 8155, 8157, 8158).

Received 24 February 2005; **Revised** 14 June 2005; **Accepted** 7 July 2005; **Published** 27 September 2005.

Sclater, J. G., N. R. Grindlay, J. A. Madsen, and C. Rommevaux-Jestin (2005), Tectonic interpretation of the Andrew Bain transform fault: Southwest Indian Ocean, *Geochem. Geophys. Geosyst.*, *6*, Q09K10, doi:10.1029/2005GC000951.

Theme: Accretionary Processes Along the Ultra-Slow Spreading Southwest Indian Ridge
Guest Editors: Catherine Mevel and Daniel Sauter

1. Introduction

[2] The introduction of the concept of the transform fault [*Wilson*, 1965], where two lithospheric plates undergoing generation slide past each other, provided the key insight to the quantitative development of the theory of plate tectonics [*McKenzie and Parker*, 1967; *Morgan*, 1968]. Large-offset transform faults such as the Romanche (900 km, the longest in the oceans) in the central Atlantic formed the basis of this concept. Most oceanic transform boundaries consist of a single, discrete, narrow strike-slip zone offsetting two mid-ocean ridge segments [*Fox and Gallo*, 1984]. Modern satellite altimetry and high-resolution swath-mapping, however, have revealed that the Romanche and a similar large-offset transform in the Southwest Indian Ocean, the Andrew Bain (750 km, second longest in the oceans), have complex multifault geometries and do not lie on small circles about the Eulerian pole of rotation [*Cande et al.*, 1988; *Shaw and Cande*, 1990; *Chu and Gordon*, 1999]. In recognition of the unique structural framework of these large age-offset transforms, *Ligi et al.* [2002] propose that both the Romanche and Andrew Bain represent a new class of oceanic transform boundary called megatransforms.

[3] Counterclockwise plate motion changes put a left lateral transform fault into extension. This concept has given rise to a number of models to account for the occurrence of broad regions of deformation both within and bordering large oceanic transforms. These include the "leaky" transform fault concept [*Menard and Atwater*, 1969] with the creation of a single intratransform spreading center [*Pockalny et al.*, 1997] or several intratransform spreading centers sandwiched between multiple closely spaced transform faults [*Searle*, 1983] with the propagation of the ridge tips across the transform valley creating a more complex morphological pattern [*Tucholke and Schouten*, 1988]. Also, these models embody extensional transform zones [*Taylor et al.*, 1994], characterized by overlapping en echelon volcanic systems and a diffuse band of earthquakes. Major strike-slip features on land are generally complicated structures and their motion is not purely lateral. This can give rise to pull-apart basins or diffuse "relay zones" [*Aydin and Nur*, 1982]. *Searle* [1983] and *Garfunkel* [1986] have argued that such features could contribute to increasing the width of major oceanic transform faults. On the slowly spreading Southwest Indian Ridge (SWIR), *Sauter et al.* [2001] and *Dick et al.* [2003] have observed segments of oblique crustal accretion. The occurrence of such accretion within the transform domain would significantly increase the apparent width of a transform fault.

[4] All of the above concepts involve a change in direction of spreading or oblique spreading to create the space that permits the transform fault to widen. *Ligi et al.* [2002] have proposed an alternative model that does not involve either of these phenomena. They have suggested that difficulties in faulting the cold, strong lithosphere in the center of the transform domain create two symmetric strike-slip faults that isolate a lens shaped zone of oceanic lithosphere within the transform domain of a large age-offset transform fault. They applied this concept to account for the morphology of the Romanche transform fault and have suggested that the excessive width of the large age-offset Andrew Bain transform fault might have the same explanation.

[5] In the austral summer of 1996, we carried out a high-resolution swath-mapping and shipboard gravity and magnetic survey of the ultra-slow spreading (14–16 mm/yr full rate) SWIR between 15°E and 35°E [*Grindlay et al.*, 1996, 1998]. This survey (KN145L16) included four lines within the Andrew Bain transform domain. In this paper, we present the regional background, and combine this with the survey data and local seismicity to provide a morphotectonic interpretation of the transform domain. We discuss the possible models that can account for both the complex geometry and the excessive width of the domain. We finish by providing a conceptual tectonic history of the Andrew Bain

transform fault over the past twenty million years.

2. Regional Background

2.1. Southwest Indian Ridge

[6] The ultra-slow spreading SWIR, with a pronounced depression delineating the axis, dominates the floor of the southwestern Indian Ocean. The ridge extends 7700 km from the Bouvet triple junction at 55°S, 0°E to the Rodrigues triple junction at 25°S, 70°E [*Fisher et al.*, 1982; *Fisher and Goodwillie*, 1997]. The ridge marks the divergent boundary between the Antarctic and the Nubia and Somalia plates. A series of fracture zones cross cut the SWIR. *Fisher et al.* [1986] explored, delineated and sampled by dredging the four most prominent: the Du Toit, Andrew Bain and the dual Prince Edward fracture zones. *Sclater et al.* [1997] suggested that the western deep of the dual Prince Edward fracture zone be renamed "Marion Fracture Zone." We employ this name for the rest of this paper.

[7] Collectively the Du Toit, Andrew Bain, Marion and Prince Edward fracture zones offset less than 400 km of ridge axis left-laterally by nearly 1230 km and divide the SWIR into two almost equally long sections. These fracture zones reveal the relative motion of Africa with respect to Antarctica nearly back to the break-up of these two continents in the Late Jurassic. The greater than 2:1 ratio, cumulative ridge axis offset to the total axial spacing of the four fracture zones, is comparable to the fracture zone dominated equatorial part of the Mid-Atlantic Ridge [*Searle et al.*, 1994] and to Eltanin and adjacent fracture zones in the South Pacific [*Lonsdale*, 1994].

[8] The trace of the Andrew Bain Fracture Zone extends from the southern end of the Mozambique Escarpment via the Astrid Ridge (M and A, inset, Figure 1) almost to the continental shelf off Antarctica. The long, wide transform domain of the Andrew Bain marks the western boundary of the "Marion Swell," a large region of elevated seafloor topography, lying between the Madagascar Plateau and the Del Cano Rise (MP and DCR, inset, Figure 1), that stretches from 35°E to 50.5°E [*Fisher and Goodwillie*, 1997]. The active section of the Andrew Bain Fracture Zone represents the longest age-offset (56 million years) and the greatest width (120 km) of any transform fault in the oceans (Figure 1). The most powerful strike-slip earthquake (111042 Ms 8.1, Table 1) on any oceanic transform fault occurred in 1942 in the center of the Andrew Bain [*Okal and Stein*, 1987].

2.2. Tectonic History of the Southwest Indian Ocean

[9] Magnetic anomalies indicate that seafloor spreading has occurred between Africa [*Segoufin*, 1978; *Simpson et al.*, 1979] and Antarctica [*Bergh*, 1977; *LaBrecque and Hayes*, 1979] since the Late Jurassic. Africa first separated from Antarctica in a northward direction and then, sometime in the quiet zone (before 84 Ma, Chron 34), changed direction of motion to northeastward. However, between 69 and 56 Ma (Chrons 31y to 24o), another change in direction occurred and Africa moved northwestward with respect to Antarctica. At 56 Ma (Chron 24) Africa returned to its prior direction of motion and again moved steadily northeastward until sometime in the Miocene [*Royer et al.*, 1988]. These changes create the striking S-shaped features on the satellite-derived gravity and tectonic charts (Figure 1 and inset).

[10] In the early Miocene, the African plate split along the East African Rift into the Nubia and Somalia plates [*Ebinger et al.*, 2000]. *Lemaux et al.* [2002] have argued that the Nubia/Somalia plate boundary at 11 Ma (Chron 5o) is almost entirely strike-slip and meets the SWIR at the eastern end of the Andrew Bain transform fault. Younger than 3.2 Ma (Chron 2A) the boundary becomes more diffuse [*Chu and Gordon*, 1999] and it is not known where it meets the ridge axis.

3. Data

3.1. Multibeam Bathymetry

[11] We ran four long multibeam profiles close, and parallel to the trend of, the transform fault (Figure 1). We collected both bathymetry and side scan sonar data with a SeaBeam 2112 multibeam system and gridded the data at a 250 m interval. Unfortunately, poor quality prevented the use of the side scan sonar data in the morphotectonic analysis of the transform domain. For a view of the entire Andrew Bain transform domain (Figure 2), we merged digital depths from the multibeam with a gridded version of the composite single-beam contour chart of *Fisher and Goodwillie* [1997].

[12] An 80- to 120-km-wide swath of rough topography characterizes the Andrew Bain transform fault between the southwestern ridge-transform

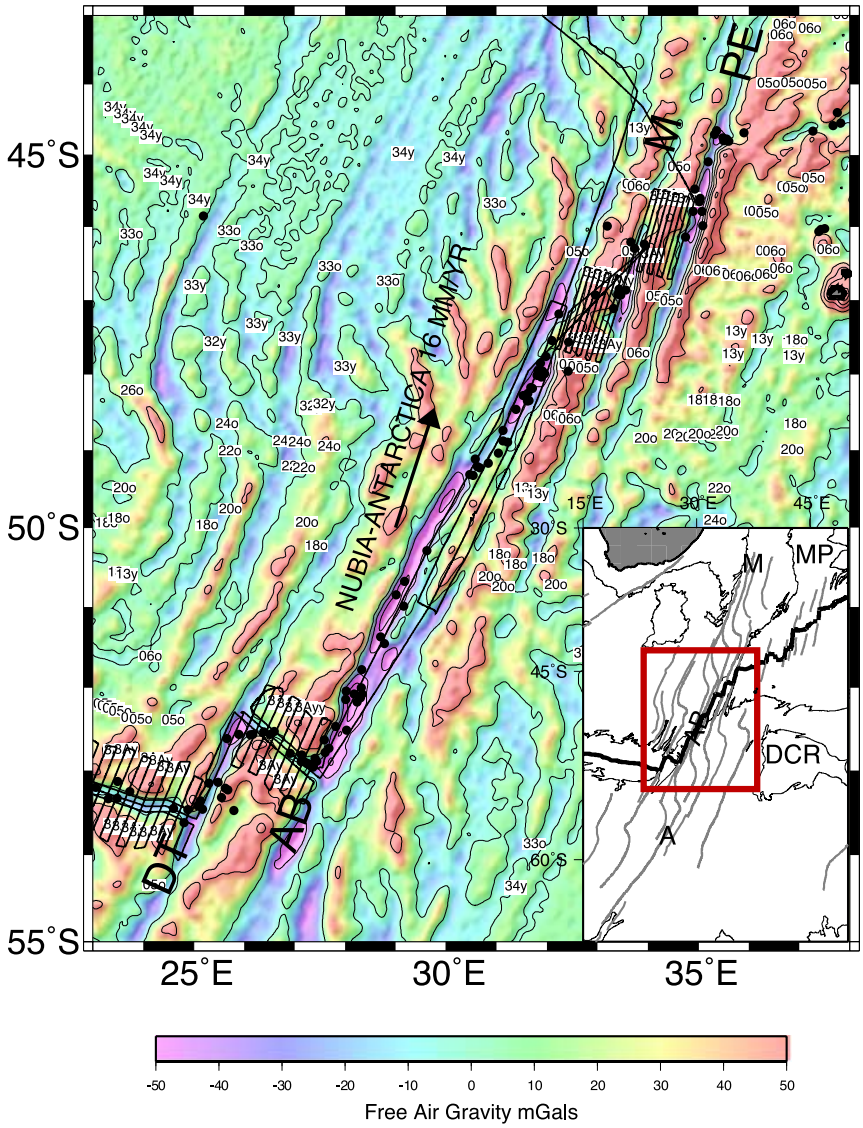

Figure 1. The Andrew Bain and associated transform faults offsetting the SWIR. Relocated earthquakes (black dots) [*Engdahl et al.*, 1998] and the KNORR145L16 track (black lines) superimposed upon the satellite-derived free air gravity field of the area [*Sandwell and Smith*, 1997]. DT, AB, M, and PE identify Du Toit, Andrew Bain, Marion, and Prince Edward transform faults, respectively. The small numbers on a white background represent the position of identified magnetic anomalies 3Ay and older. The arrow indicates the separation direction of Nubia plate from the Antarctica plate [*Chu and Gordon*, 1999]. (inset) Crest of the SWIR (thick black line) and the traces of the prominent fracture zones (shaded lines) superimposed upon the 4000 m contour (thin black line) in the Southwest Indian Ocean [after *Sclater et al.*, 1997]. M, A, MP, and DCR represent Mozambique Escarpment, Astrid Fracture Zone, Madagascar Plateau, and Del Cano Rise, respectively. The red box represents the area covered by Figure 1.

intersection (RTI) at 52°50′S, 27°40′E and the northeastern RTI at 47°10′S, 32°35′E (Figure 2). This swath represents the transform domain. A 450-km-long, 20-km-wide valley trending north-northeast from the southern RTI marks the southwestern boundary of the domain. Just to the east, a number of narrower corrugations run up the center of the domain before terminating in a series of deep overlapping basins (TRZ, Figure 2) that connect via a 10-km-wide, 100-km-long north-northeast trending valley to the northern ridge-transform intersection (RTI). The eastern central portion of the domain contains an en echelon series of narrow (10- to 15-km-wide, 50- to 70-km-long) elongate ridges and troughs (ERT, Figure 2) that range in orientation between N40°E and N60°E. They lie at roughly 10° to 30° to the direction of separation of Nubia/Antarctica. The northern sector of the do-

Table 1. Source Parameters for the Earthquakes Shown in Figures 1, 2, 3, and 4

Event	Lat.	Long.	Str.	Dip	Rake	mb	Ms	Mo[a]
			Okal and Stein [1987]					
111042[b]	−49.4	30.6	196	84	−168	7.7	8.1	1300
			Body Wave Inversion [*Wald and Wallace*, 1986][c]					
022564[d]	−44.66	37.27	357	68	−172	6.7		22
060868[b]	−48.88	31.13	213	72	−156	5.6	6	2.4
072469[e]	−45.65	35.03	189	83	175	5.7	5.9	3
102669[d]	−53.33	23.48	75	52	−125	5.9	6.1	4.7
021973[e]	−45.61	35.04	199	78	−175	5.5	5.6	3.8
050974[e]	−45.98	35.09	197	81	−151	5.7	5.9	2.5
082178[b]	−47.57	32.43	205	88	178	5.8	6.2	3.7
111180[b]	−51.37	28.71	223	78	−112	6.2	6.7	22
011282[b]	−52.52	28.03	205	68	−178	5.8	5.7	1.7
			CMT – Poor[f]*Double Couple Solutions* [*Dziewonski et al.*, 1983–1999][c]					
100884A[b]	−47.96	31.91	60	72	−98	5.4	5.3	0.35
111687B[b]	−49.32	30.47	40	52	−141	5.5	4.3	0.13
082795A[b]	−47.99	31.96	206	77	−162	5.1	4.7	0.07
			CMT – Reliable Double Couple Solutions [*Dziewonski et al.*, 1983–1999][c]					
120877B[b]	−52.04	28.03	19	65	−178	5.1	4.8	0.13
081078E[d]	−44.55	37.83	86	44	−71	4.9	4.9	0.16
082678A[b]	−47.19	32.24	19	69	−168	4.7	5.3	0.26
110281B[d]	−52.92	27.26	110	58	−94	5.2	5.2	0.38
060783A[b]	−50.68	29.18	212	76	−134	5.5	5	1.1
072683B[e]	−44.77	35.56	12	87	−158	4.9	5.2	0.41
080383A[b]	−52.14	28.02	20	84	−180	5.5	5.4	0.62
090183A[g]	−52.57	25.9	200	87	−175	5.4	5.9	2.8
022584B[b]	−47.95	31.83	227	21	−123	5.5	5.6	0.5
060684C[b]	−48.35	31.65	202	90	165	5.4	4.8	0.09
041185B[g]	−53.32	25.55	26	67	−173	5.1	5.1	0.36
051585A[b]	−51.78	28.34	204	81	−161	5.6	5.4	0.41
111186B[b]	−48.89	31.22	204	88	176	5.7	5.8	1.3
011687C[d]	−52.89	27.44	66	71	−102	5.5	4.8	0.25
112587B[g]	−53.62	24.81	203	90	162	4.8		0.09
080988A[e]	−44.75	35.49	192	78	170	5.2	5.2	0.25
031191C[b]	−50.99	29.16	207	84	−176	5.7	6.3	0.45
050692C[e]	−45.79	34.9	184	90	−180	5	4.6	0.07
011993A[e]	−45.09	35.20	197	80	175	5.1	5.6	0.75
032993E[d]	−52.96	27.36	88	51	−115	5.7	5.3	0.44
060293A[h]	−46.3	33.75	15	72	177	5.2	5.6	0.6
102293A[d]	−52.8	26.92	91	24	−129	5.3	4.9	0.1
070394C[b]	−48.28	31.53	183	53	170	5.1	4.8	0.13
040896C[d]	−52.82	27.14	114	28	−113	5.1		0.07
080897A[d]	−44.65	35.37	91	45	−78	5	4.6	0.05
122997A[b]	−52.08	28.18	22	79	168	5.1	5.3	0.41
			CMT – Reliable Double Couple Solutions [*Dziewonski et al.*, 2000–2003; *Ekstrom et al.*, 2003]					
060399A[b]	−48.37	31.46	8	88	−147	5		0.13
110299C[g]	−52.85	25.87	202	87	178	5	5.1	0.14
031700B[g]	−53.01	26.28	23	80	−175	5	5.2	0.32
031700D[g]	−52.89	25.56	198	90	−180	4.9		0.05
092500A[d]	−46.59	37.56	3	84	0	5.6	5.6	0.74
021801B[b]	−47.17	32.55	15	84	−171	5.5	5.7	1.2
121301G[d]	−53.73	25.35	116	44	−114	5.3	5	0.07
121401D[d]	−53.38	25.23	138	38	−92	5.2	5.2	0.22
121401E[d]	−53.56	25.41	142	41	−85	5	5.1	0.1

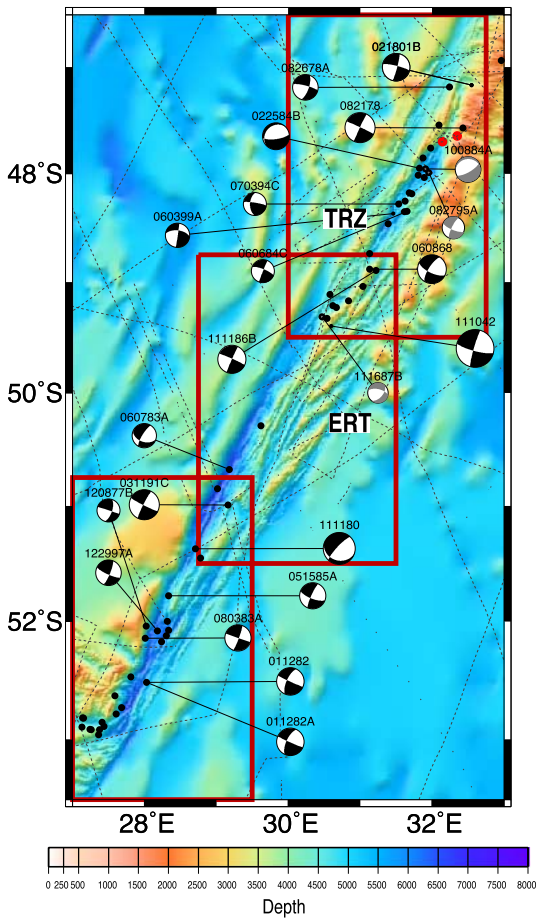

Figure 2. Relocated earthquake epicenters (black dots), focal mechanism solutions (beach balls, size indicates relative magnitude) (*Wald and Wallace* [1986]; *Dziewonski et al.* [1983–1999, 2000–2003]; *Ekstrom et al.* [2003]), and dredge locations (red dots) superimposed upon a topographic chart constructed by merging [*Goodwillie*, 1996] the KN145L16 multibeam data with a gridded version of the single beam contour chart of *Fisher and Goodwillie* [1997] (TRZ, transform relay zone; ERT, en echelon ridges and troughs). The dotted lines represent single beam ship tracks. The small dots give the unrelocated position of the post-1998 focal mechanism solutions. The red lines enclose the northern, central, and southern sectors presented as Figure 4.

main marks the westernmost extent of the thermal signature of the "Marion Hot spot" along the SWIR [*Georgen et al.*, 2002]. This signature gives rise to roughly 1.5 km shallower depths within the domain in the vicinity of the northern relative to the southern RTI.

3.2. Seismicity and Earthquake Focal Mechanisms

[13] The Harvard centroid moment tensor (CMT) catalog [*Dziewonski et al.*, 1983–1999, 2000–2003; *Ekstrom et al.*, 2003] contains solutions for thirty-nine earthquakes that occurred between 23° and 38°E from 1976 to January 2002 along the SWIR. *Wald and Wallace* [1986] and *Okal and Stein* [1987] using body wave inversion techniques and analysis of long-period surface waves, respectively, provide another ten solutions (Table 1). To evaluate the CMT solutions, we followed *Nettles and Ekstrom* [1998] and examined the eigenvalues of the moment tensor. The parameter ε, that describes the size of the non-double-couple component of the moment tensor, is related to the diagonals of the moment tensor in the principal axis coordinate system. For a pure double-couple moment $\varepsilon = 0$, while for a compensated linear-vector dipole $\varepsilon = \pm 0.5$. Only three of the 39 CMT solutions had ε values greater than 0.3. We plotted these three less-reliable solutions in light gray (Figure 2). For consistency, we use the position of the relocated earthquake epicenters from *Engdahl et al.* [1998] for the location of the body wave mechanisms and the pre-1999 CMT solutions on all charts. We provide these locations in Table 1.

[14] We compared International Seismic Centre, National Earthquake Information Center, and relocated earthquake positions from *Shearer* [2001] and *Engdahl et al.* [1998] with prominent features on the ocean floor. We found the locations of *Engdahl et al.* [1998] and *Shearer* [2001] to be equally consistent with the ocean floor features. Because they are more generally available, we chose to use the relocated locations of *Engdahl et al.* [1998]. *Engdahl et al.* [1998] estimated the error in the epicentral position for their shallow earthquakes on land to be about 10 km. The error in this position for earthquakes in the Southeast Indian Ocean is probably somewhat larger than 10 km due to the scarcity of nearby local stations.

Notes to Table 1:

[a] Seismic moment given in 10^{25} dyn cm.
[b] Andrew Bain Transform Fault.
[c] Location from *Engdahl et al.* [1998].
[d] Southwest Indian Ridge.
[e] Prince Edward Transform Fault.
[f] According to the criteria of *Nettles and Ekstrom* [1995].
[g] Du Toit Transform Fault.
[h] Marion Transform Fault.

Table 2. Comparison of the Observed Azimuth in Degrees Shown by Topography and the Slip Vectors Derived From the Focal Mechanisms for the Andrew Bain and Adjacent Transform Faults With the Azimuth Predicted by Nouvel1 [*DeMets et al.*, 1990] for Africa/Antarctica, and *Chu And Gordon* [1999] for Nubia/Antarctica and Somalia/Antarctica Plate Motions

				Slip Vectors		Predicted Azimuth		
Transform Faults	Lat., S	Long., E	Obs. Az.	Number	Mean	Afr/Ant[a]	Nu/Ant[b]	Som/Ant[c]
Du Toit	53	25.5	22 ± 3	6	22 ± 3	24	22	11
Andrew Bain	50	30	28 ± 3	15	20 ± 7	20	18	9
Marion	46.5	33.6	15 ± 5	-	-	17	15	7
Prince Edward	45.4	35.1	14 ± 3	8[d]	13 ± 5	15	13	7

[a] Africa – Antarctica, 5.6°N, 39°W [*DeMets et al.*, 1990].
[b] Nubia – Antarctica, 1.9°N, 38.5°W [*Chu and Gordon*, 1999].
[c] Somalia – Antarctica, 5.6°N, 65.6°W [*Chu and Gordon*, 1999].
[d] Marion and Prince Edward combined.

[15] At the spreading centers, the epicenters lie within the central rift valley. On the Du Toit, Marion and Prince Edward transform faults the earthquakes plot within the single transform valley marking these features (Figure 1). In the southern section of the Andrew Bain the epicenters follow the southwestern valley; they cross over the domain via a suite of deep overlapping basins (TRZ, Figure 2) before following the northeastern deep to the northern RTI at 47°10′S, 32°35′E. All of the focal mechanisms on the Du Toit, Marion and Prince Edward transform faults give strike-slip solutions. In contrast, while seventeen of the twenty-two mechanisms within the Andrew Bain transform domain gave strike-slip solutions, five show a significant component of dip-slip faulting.

[16] We compared the slip vectors of the strike-slip earthquakes and the azimuth of the actual transform faults with those predicted for Nubia/Antarctica and Somalia/Antarctica relative plate motion [*Chu and Gordon*, 1999] (Table 2; Figure 3). The Du Toit, Marion and Prince Edward transform faults have average slip vectors and azimuths far from that predicted by Somalia/Antarctica motion but within 2° of that predicted for Nubia/Antarctica plate motion [*Chu and Gordon*, 1999] (Table 2). We argue that between Chron 2A (3.2 Ma) and the present, the western edge of the zone of distributed extension comprising the Nubia/Somalia plate boundary must lie to the east of the Prince Edward transform fault. Thus the analysis of *Lemaux et al.* [2002] and these observations of the azimuth of the transform faults place the Andrew Bain transform fault entirely on the Nubia/Antarctica plate boundary from at least 11 Ma (Chron 5o) to the present.

3.3. Magnetic Data

[17] We collected magnetic data on the 1996 survey using a Geometrics G-886 marine magnetometer towed between 250 and 350 meters behind the ship. We logged the total field at 8 sec intervals for most of the cruise and computed the magnetic anomaly by removing the International Geomagnetic Reference field. We superimposed the magnetic anomaly profiles from KN145L16 on the gridded topography of the Andrew Bain transform domain. We observed anomalies as great as 1000 nT over the spreading centers. However, within the Andrew Bain transform domain they were generally less than 50 nT except for a single 150 nT anomaly at 49°15′S, 30°40′E. This anomaly occurred over the southern scarp of the seismically active deep overlapping basins. Neither these profiles, nor two shorter profiles run earlier by H. W. Bergh (personal communication (1996) presented by *Sclater et al.* [1997]) provide any evidence for either recognizable magnetic anomalies or magnetic lineations within the transform domain.

3.4. Satellite Gravity Data

[18] The axis of the SWIR shows up as a distinct (20 mGal) low on the free air satellite gravity field [*Sandwell and Smith*, 1997] except immediately to the east of the Prince Edward transform fault (Figure 1). Alternating, closely spaced positive and negative free air gravity anomalies initially trending parallel to the transform faults extend out from the ridge axis. The highs reflect normal ocean floor and the lows the fracture zone continuations of the transform faults. The major change in Africa/Antarctica motion between Chrons 24o and 31y (56 Ma and 69 Ma) creates the short positive lineations that lie oblique to the general trend. These lineations are symmetric about the axis of the SWIR.

[19] A 50-km-wide and strikingly linear 50 to 100 mGal negative free air gravity anomaly marks

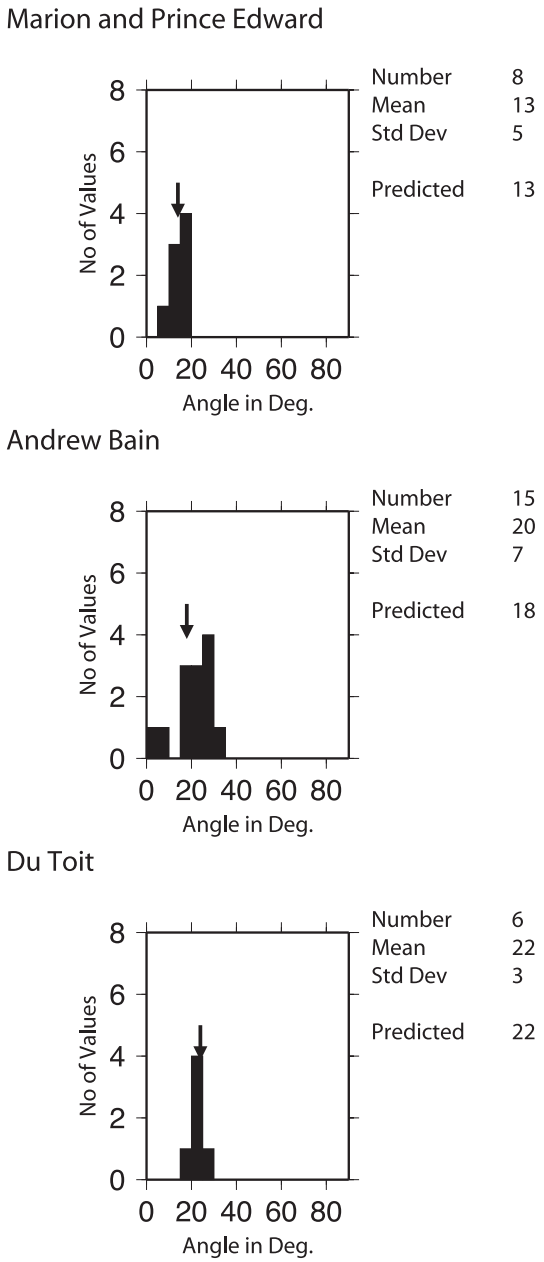

Figure 3. Histogram of slip vectors for the earthquake focal mechanism solutions from the (bottom) Du Toit, (middle) Andrew Bain, and (top) combined Marion and Prince Edward transform faults. The text compares the mean and standard deviation of the slip vectors with the predicted direction of separation of the Nubia plate from the Antarctica plate from *Chu and Gordon* [1999]. The arrows above the histograms identify the predicted separation direction.

the western valley of the Andrew Bain transform domain and the seismically active overlapping basins that cross the domain (Figure 1). The en echelon ridge-and-trough topography in the eastern section of the domain is characterized by 30 to 50 mGal positive gravity anomalies. These anomalies have the same magnitude as the positive gravity anomalies that characterize the ocean floor on either side of the transform domain.

3.5. Rock Types

[20] Only two rock dredge hauls have been recovered from the entire length of the Andrew Bain transform domain [*Fisher et al.*, 1986] (red dots, Figure 2). The dredges lie on the eastern side of a narrow 100-km-long north-northeast trending valley just south of the northern ridge-transform intersection (Figure 2). They were taken close together and depth controlled. The first (PROTEA 15 at 47°42′S, 32°09′E) started at 4400 m and ended at 4000 m depth and the second (PROTEA 16 at 47°39′S, 32°21′E) started at 2500 m and ended at 2260 m depth. They represent a partial section of the eastern flank of the valley. The first dredge haul yielded predominantly peridotite and basalt, the second gabbro and peridotite. These rocks are consistent with this valley marking a transform fault that has exposed a section of normal ocean plutonic crust created at a slow spreading ridge. The lack of any other dredge hauls prevented us from using rock type further to aid our tectonic interpretation of the rest of the transform domain.

4. Results

4.1. Northern Sector

[21] A 20-km-wide valley cutting into a region of generally elevated topography (3000 m) outlines the northern spreading center (Figures 4a and 4b). The RTI occurs where this valley intersects a 20-km-long north-south trending deep (4500 m) at 47°10′S, 32°20′E (A, Figure 4b). Immediately south of this deep lies a 10-km-wide valley bounded on the west by a ridge and on the east by oceanic crust created at a spreading center which is recognized by its prominent abyssal hill fabric. Within this valley lies an elongate region of elevated topography. A narrow 1- to 2-km-wide cleft starting at the RTI (A, Figure 4b) runs down the center of this elevated region (northwestern inset, Figure 4a) and continues on to the south as a valley before terminating at the northeastern edge of a deep (5500 m) basin at 47°40′S, 32°10′S. (Figure 4a; B, Figure 4b). Three large earthquakes with strike-slip focal mechanisms (021801B, 082678A and 082178) occur within 15 km of the cleft and the valley (Figure 4b).

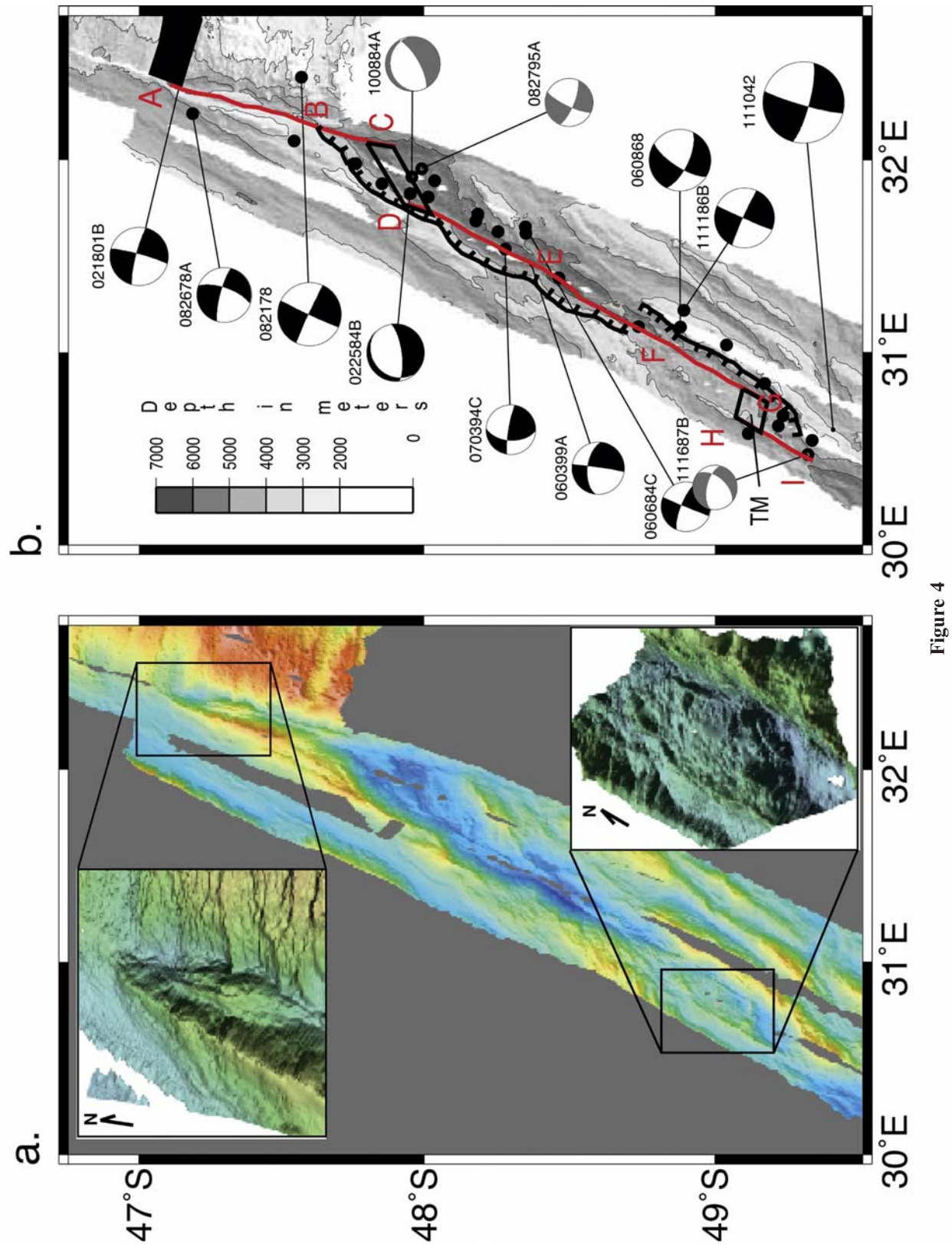
a.
47°S
48°S
49°S
30°E
31°E
32°E
N
b.
A
B
C
D
E
F
G
H
I
TM
021801B
082678A
082178
022584B
100884A
082795A
070394C
060399A
060684C
111687B
060868
111186B
111042
Depth in meters
0
2000
3000
4000
5000
6000
7000

Figure 4

[22] Three seismically active interconnected basins lie south-southwest of the valley (Figure 4b). The northern basin, mentioned above, is the broadest with a width of 30 km and a length of 50 km. The central basin is narrower, varying in width between 10 and 20 km. Also it is longer with a length of roughly 100 km. Both of these deep basins are flanked on the north and west by ridges with southeastward dipping, arcuate, steep scarps. The shallower (4000 m) southern basin is bounded on the southeast by a 50-km-long northwestward dipping arcuate scarp (Figure 4a). Two high angle dip-slip solutions (100884A and 022584B) and one strike-slip solution (082795A) lie within the northernmost basin (Figure 4b). Three strike-slip solutions (070394C, 060399A, 060684C) fall within or very close to the central basin. Two other strike-slip solutions (060868 and 111186B) are located on top of the steep northwestward facing slope near the junction of the central and southern basins (Figure 4b). Seven relocated earthquakes lie within or very close to the southern basin. Two occur within the actual basin and the five others fall close to the crest of the arcuate scarp at the southern end. Only one of these earthquakes yielded a fault plane solution, a normal-fault (111687B) with a 52° dip (Figure 4b).

[23] A detailed examination of the shaded relief chart of the floor of the three basins (Figure 4a) reveals some subtle but potentially important features that trend either roughly parallel to, or, approximately at right angles to the spreading direction. The trend of the cleft in the northeastern valley can be continued south well into the northern basin. There, the trace connects to an elevated mound at 47°52′S, 32°05′E (C, Figure 4b) that crosses the basin in a southwesterly direction before connecting up with a narrow ridge (D, Figure 4b) that runs down the eastern side of the northern section of the central basin. The linear trend appears to cross the basin at 48°30′S, 31°25′E (E, Figure 4b) and reappear as a valley that runs down the eastern side of the southern section of the central basin. Though interrupted by a southerly trending topographic mound at 48°50′S, 31°05′E (F, Figure 4b) this ridge and valley sequence lines up with a narrow linear ridge on the eastern side of the southern basin. The ridge in the southern basin terminates at 49°08′S, 30°48′E (G, Figure 4b) against a short mound with a cleft in the middle (TM, Figure 4b) that makes a westerly crossing of the basin (southeastern inset, Figure 4a). In turn, this mound abuts against another narrow ridge (H, Figure 4b) that exits the southern basin in a south by southwest direction. This ridge can be traced as far south as 49°20′S, 30°28′E (I, Figure 4b).

4.2. Central Sector

[24] The western multibeam line identified the eastern side of a 5000 m to 6000 m-deep valley that runs north-northeast up the entire length of the central sector before terminating at 49°20′S, 30°20′E, very close to the narrow ridge that exits the southern basin of the northern sector (Figure 4c; I, Figure 4d). This line did not delineate the western wall of this valley. However, inspection of the

Figure 4. (a) A colored shaded relief image of the KN145L16 multibeam data (gridded at 200 m in longitude and 300 m in latitude and spline interpolated to 1 km in longitude and 1.5 km in latitude) within the northern sector of the Andrew Bain transform domain. See Figure 2 for contour color scheme. The northeastern inset provides a perspective image of the northern RTI and PTDZ; the southeastern inset provides the southern relay basin. Both illuminated from the northwest. The data were regridded at 150 m and have a vertical exaggeration of 4:1. Produced using *Fledermaus* from IVS-3D. (b) Tectonic interpretation. Relocated earthquake epicenters (black circles) and focal mechanism solutions (beach balls, size indicating relative magnitude: black, reliable; gray, less reliable) superimposed upon generalized contours and major tectonic elements (black rectangles, spreading center; open rectangles, zones of accretion within relay basins; continuous black lines, transform faults; hatched lines, rifted scarps dipping steeply in the direction of the hatch). Lines ABC, DEFG, and HI mark the predicted position of the PTDZ; see text for explanation. TM identifies a westerly trending topographic mound. See Figure 2 for overall location of sector. (c) A colored shaded relief image of the KN145L16 multibeam data (gridding as for Figure 4a) within the central (en echelon ridge-and-trough) sector of the Andrew Bain transform domain. See Figure 2 for contour color scheme. The inset provides a perspective image of the central trough of the southern en echelon ridge-and-trough morphology illuminated from the southeast. Data preparation as for the insets in Figure 4a. (d) Tectonic interpretation. Symbols as for Figure 4b. Line HI marks the possible position of the PTDZ. AB identifies the position of a long narrow ridge discussed in the text. See Figure 2 for overall location of sector. (e) A colored shaded relief image of the KN145L16 multibeam data (gridding as for Figure 4a) within the southern sector of the Andrew Bain transform domain. See Figure 2 for contour color scheme. The inset provides a perspective image of the southern RTI illuminated from the southeast. Data preparation as for Figure 4a. (f) Tectonic interpretation. Symbols as for Figure 4b. Lines AB and CD mark the possible position of the PTDZ. See Figure 2 for overall location of sector.

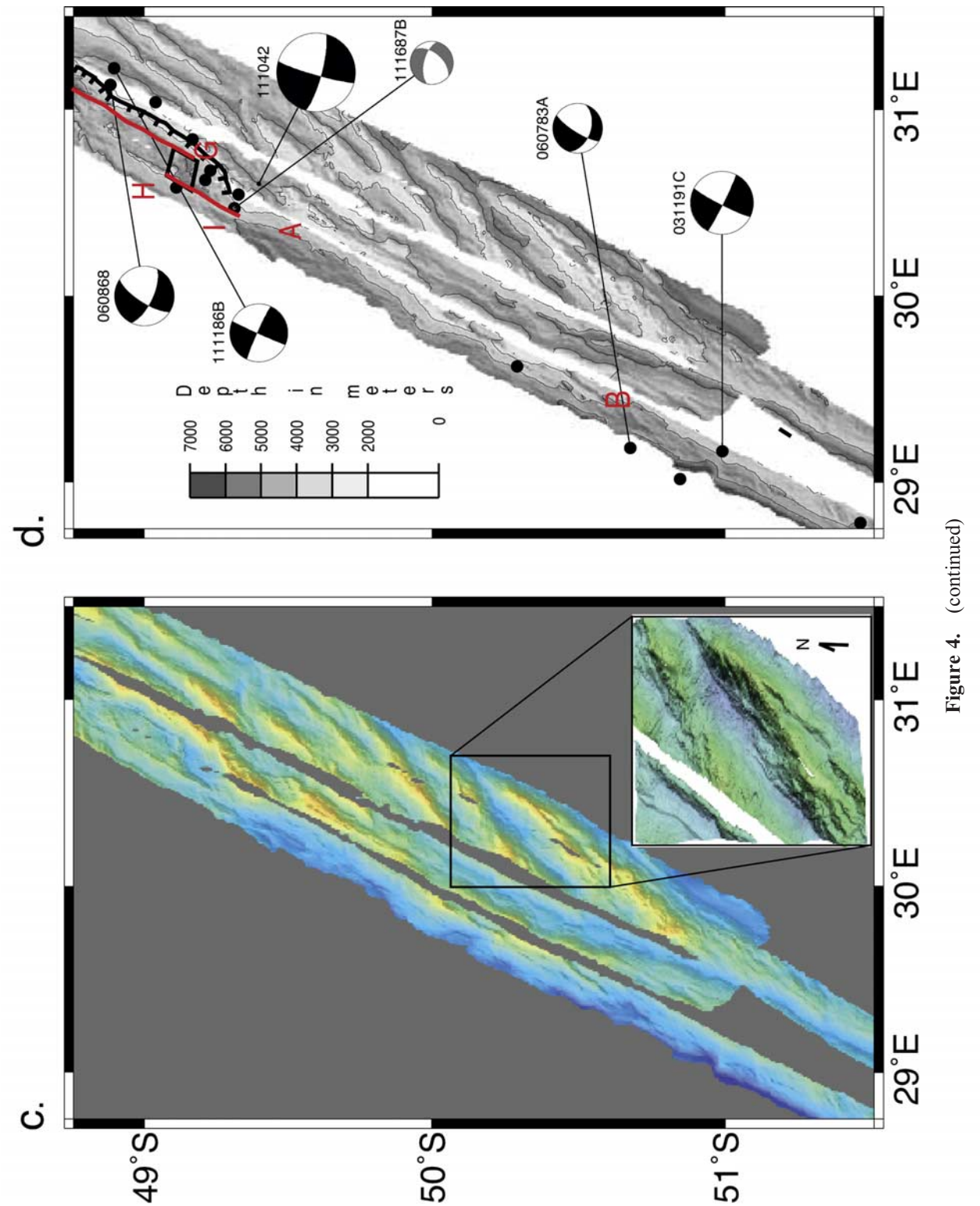

Figure 4. (continued)

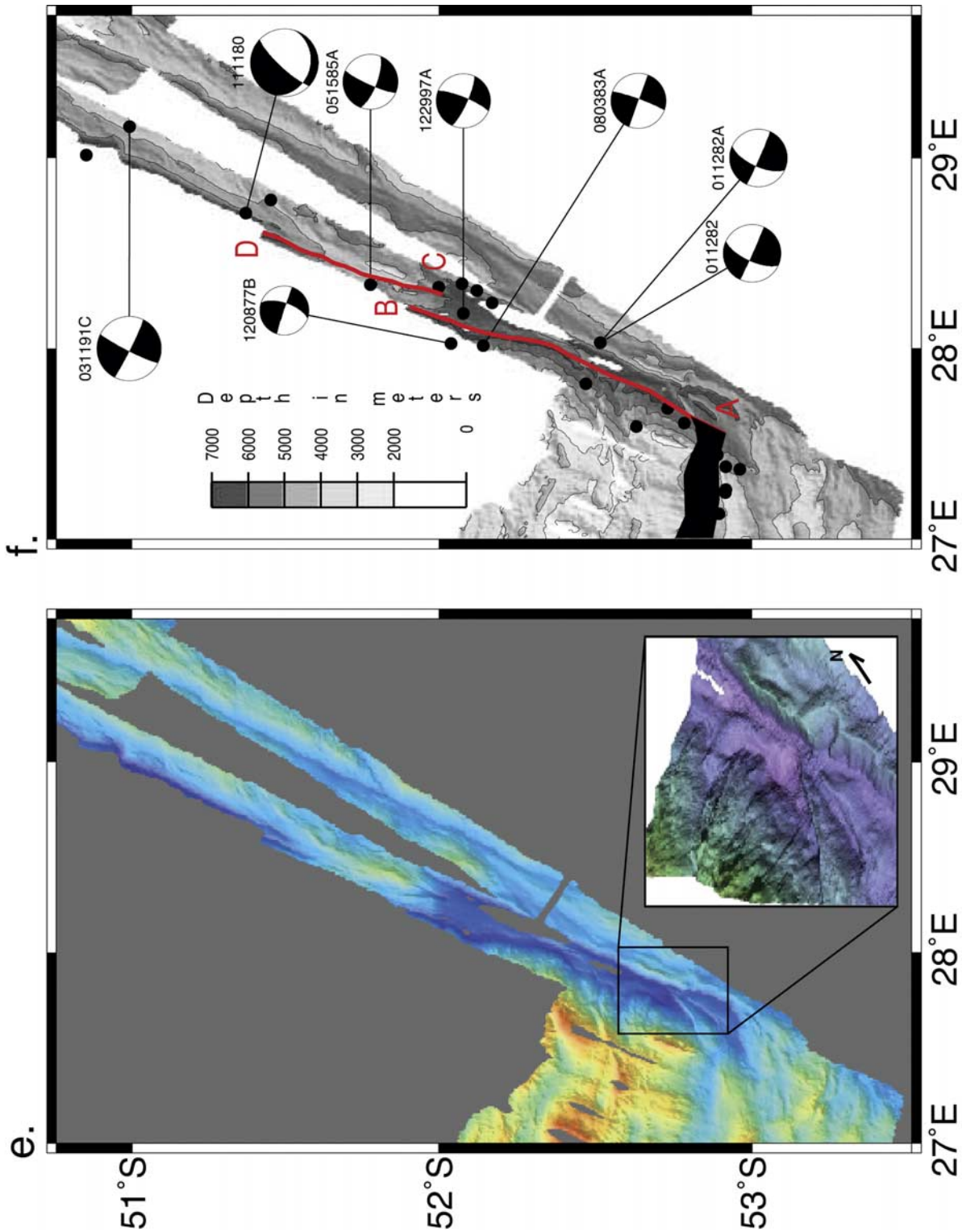

Figure 4. (continued)

generalized chart of the transform domain (Figure 2) shows that the western flank starts about 5 km to the west of the line and that this flank marks the western wall of the domain. An en echelon suite of seven ridges and troughs lying between 48°30′S (Figure 4a) and 51°00′S (Figure 4c) occupies almost the entire eastern side of the sector (ERT, Figure 2). The southern four ridges trend 30°E and the northern three 10°E with regard to direction of separation of Nubia/Antarctica. The southern four have a lenticular shape, with an approximate width, length, and height of 10 km, 60 km, and 1 km, respectively. The widest and deepest of the troughs lies in the center of the four ridges and its southern flank shows evidence of block faulting (inset, Figure 4c). The absence of magnetic anomalies over any of the ridges or troughs indicates that they have a very weak magnetization. A pronounced swale lies just west of the en echelon ridge-and-trough morphology and a long, narrow (20-km-wide) (AB, Figure 4d) ridge separates this swale from the deep western valley.

[25] The central sector has far fewer earthquakes than the sectors to the north and south. Only one small earthquake occurs in the 180-km-long section north of event 060783A, suggesting a gap in the seismicity. The magnitude 8.1 111042 event [*Okal and Stein*, 1987] is located at the northern end of this seismic gap (Figure 4d). All earthquakes south of this event, including two strike-slip solutions (060783A and 03191C), lie within the deep western valley.

4.3. Southern Sector

[26] An east-west trending asymmetric valley (Figures 2, 4e, and 4f) between two regions of elevated topography marks the position of the southern spreading center. This spreading center spills out onto the deep floor of the valley running up the western side of the domain as a curved northeast trending ridge. A nodal deep occurs where this curved ridge intersects the southwestern continuation of this valley around 52°50′S, 27°40′E (southeast inset, Figure 4e; A, Figure 4f). The deepest section (>6500 m) of the western transform valley trends N15°E away from this curved ridge and appears to die out just north of 52°E though it may continue outside the area of data coverage (B, Figure 4f). We observe a narrow cleft running along the western side of the small ridge at 51°50′S, 28°24′E (Figure 4e; C, Figure 4f) that has the same overall trend as the deepest section of the valley to the west and south. We interpret this cleft to indicate that two closely spaced, overlapping, NNE trending deeps (AB, CD, Figure 4f) rather than one continuous feature make up the deepest sections of the southern part of the western valley (Figure 4f).

Table 3. Comparison of the Slip Vectors From Focal Mechanisms on the Andrew Bain Transfrom Fault With the Observed Trend of the Fault and the Predicted Azimuth for Nubia/Antarctica Plate Motion [*Chu and Gordon*, 1999]

	Slip Vector		Azimuth	
Location	Number	Mean	Obs.	Pred.
53°S–47°S[a]	15	20 ± 7	28	18
47°S–48°S[b]	3	16 ± 2	15	16
48°S–49°S[c]	5	18 ± 12	25	17
53°S–51°S[d]	6	22 ± 3	20	20

[a] Overall trend of the Andrew Bain.
[b] Azimuth of transform fault at 47°30′S, 30°15′E.
[c] Azimuth of transform fault at 48°30′S, 31°20′E.
[d] Azimuth of transform fault at 52°30′S, 27°55′E.

[27] Between 51°S and the southern spreading center at 52°50′S, the seven strike-slip (031191C, 051585A, 120877B, 122997A, 080383A, 011282 and 012882A) and one 78° dip-slip event (111180) all lie within 10 km of the western valley (Figure 4f).

5. Morphotectonic Analysis

5.1. Active Transform Fault

[28] The northern RTI occurs in a deep at 47°10′S, 32°20′E. We interpret the 10-km-wide depression running south-southwest from this deep as the northern transform valley of the Andrew Bain. We suggest that the narrow cleft (AB, Figure 4b) running down the center of the valley marks the principal transform deformational zone (PTDZ) in this region (northeast inset, Figure 4a; Figure 4b). The valley has a trend of N15°E, the same as that predicted for Nubia/Antarctica motion (Table 3). It is the probable location of the three nearby strike slip earthquakes (Figure 4b).

[29] Three asymmetric basins bounded on one side by steep arcuate scarps lie south-southwest of the northern transform valley. We interpret these three successive basins and scarps as a transform relay zone similar to those observed on some continental transform faults [*Aydin and Nur*, 1982; *Searle*, 1983; *Garfunkel*, 1986]. The northern and southern basins are interpreted as dominantly extensional pull-apart basins and the central basin as a wide

transform valley with a small component of transform normal extension. We interpret the narrow linear features within the relay basins (DEFG, Figure 4b) as strike-slip faults and the deep basins between them as pull-apart features (CD and GH, Figure 4b). We suggest that the long, linear strike slip feature between the two pull-apart basins marks the PTDZ. In addition, we suggest that the thin linear ridge trending south-southwest out of the southern basin also marks the PTDZ (HI, Figure 4b).

[30] Two high angle dip-slip mechanisms, 022584B and 100884A, support our pull-apart interpretation for the northern basin. Five strike-slip mechanisms (070394C, 060399A, 060684C, 060868 and 111186B) lie within or very close to the central basin supporting our interpretation of this basin as a transform valley. These strike-slip faults show a considerable amount of scatter (Table 3) in the horizontal slip vectors. However, one of the strike-slip faults (070394C) has a dip of 53° supporting our contention for some transform normal extension in the central basin. One normal fault mechanism (111687B) on the southern scarp provides evidence in favor of our pull-apart interpretation of the southern basin.

[31] We believe that the crust within the relay zone is heterogeneous, consisting in part of stretched ocean floor and in part of ultramafic and igneous basaltic rocks that have been emplaced later into the zone [*Garfunkel*, 1986]. We looked for evidence of major basaltic intrusion by examining the magnetic anomaly profiles within the zone. We did not observe any significant magnetic anomalies over either the northern or central basins indicating that any accretion within them is probably amagmatic. The only positive magnetic anomaly, a small blip at 49°15′S, 30°40′E, is located over the southeastern scarp of the southern basin. It lies just to the east of a west trending linear topographic mound that could be a neovolcanic accretionary zone within a pull-apart basin (TM, Figure 4a). However, without further supporting evidence, we cannot be sure of this interpretation for the mound. Thus we have chosen to interpret the southern basin as the site of amagmatic accretion as is the case for the northern basin. Roughly 50–60 km of ocean floor separates the elevated topography marking the limits of the northern and southern relay basins in the direction of separation of the Nubia and Antarctic plates (Figure 4b). A spreading rate of 16 mm/yr for this motion implies that the relay basins started to form between three and four million years ago.

[32] Incomplete multibeam information makes it impossible to determine how the plate boundary continues south from the thin linear ridge running south southwest out of the southern relay basin at 49°20′S, 30°28′E (Figure 4c; I, Figure 4d). However, even though there is a gap in the seismicity with only one earthquake in the next 180 km, we believe that the active section must continue southwestward, either as a transform fault, or, another transform relay basin, into the greater than 6500 m-deep valley that runs down the western side of the domain (Figure 4c).

[33] The active fault continues along the deep western valley until it terminates at the southern RTI (inset Figure 4e; A, Figure 4f). Seven strike-slip earthquakes lie within the southern portion of this valley. Both the mean of the strike of the six earthquakes and the trend of the southernmost section of the valley lie within 2° of the direction predicted by present Nubia/Antarctica plate motion (Table 3). Tentatively, we have interpreted the southern transform fault to have two strands (AB, CD, Figure 4f) overlapping at 52°00′S, 28°10′E. Incomplete bathymetric coverage prevents a more definitive conclusion. In addition, the same lack of coverage prevents us from offering an explanation of the events with substantial dip-slip component, 111180 (Figure 4f) and 060783A (Figure 4d), which lie further north within the deep western valley.

[34] In an attempt to remove the distortion introduced at high latitudes by a standard Mercator projection, we plotted the merged multibeam and single beam topography on an oblique Mercator projection about the Chron 2A (3.2 Ma) to present pole of relative motion for Nubia/Antarctica [*Chu and Gordon*, 1999]. We added relocated earthquakes [*Engdahl et al.*, 1998] and magnetic anomaly picks from Knorr145L16 for anomalies 3Ay and from *Sclater et al.* [1997] for the older anomalies (Figure 5a). We constructed a simplified tectonic chart of the area emphasizing the spreading centers, the active transform faults and the transform relay basins (Figure 5b). On the basis of the linearity of the deep western valley and the position of the relocated earthquakes [*Engdahl et al.*, 1998] we have added a third strand to the southwestern transform fault. The three strands now extend this transform fault all the way from the southern RTI at 52°50′S, 27°40′E to at least 50°00′S, 29°40′E (Figure 5b).

[35] We interpret the active transform plate boundary of the Andrew Bain Fracture Zone as a 450-km-

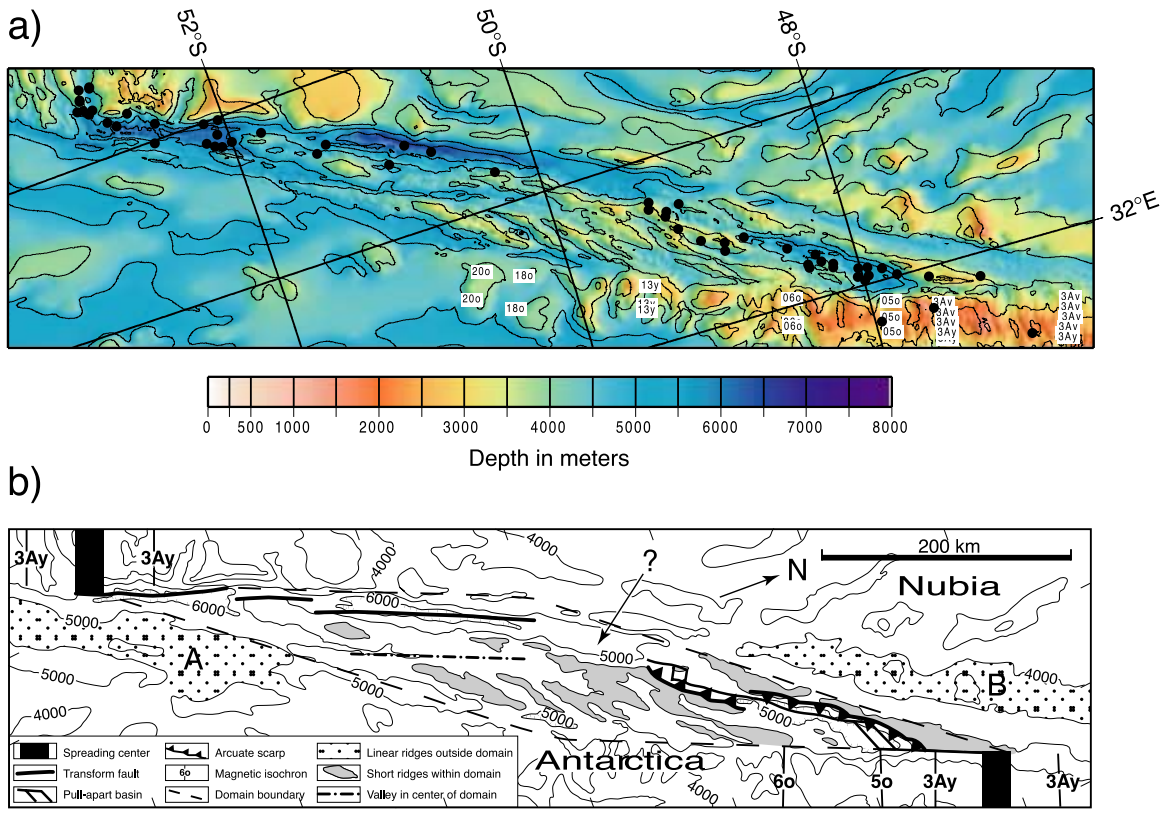

Figure 5. (a) Relocated epicenters and magnetic anomaly picks (symbols as for Figure 1) superimposed upon the merged multibeam and composite single beam topography. Oblique Mercator projection about the Nubia/Antarctica pole for Chron 2A (3.2 Ma) [*Chu and Gordon*, 1999]. (b) Simplified tectonic interpretation superimposed on a 1000 m contour chart of the area around the Andrew Bain transform fault. The dash-dot line emphasizes the valley lying west of the series of en echelon ridges and troughs.

long transform region consisting of three closely spaced overlapping strike-slip faults in the southwest connected via a three basin transform relay zone to a single 100 km strike-slip fault in the northeast (Figure 5b). However, we do not have enough information to determine how the northernmost of the three overlapping strike-slip strands connects to the transform relay zone (question mark in Figure 5b). For the southern and northern strike-slip faults, the trend and the strike of the earthquake slip vectors (Table 3) lie within 2° of the direction of relative motion of Nubia/Antarctica. Within the transform relay zone, our proposed PTDZ trends at about 8° to this direction. In addition, the scatter in the data (Table 3) prevents us from determining whether or not the earthquake slip vectors within the relay zone follow either the trend of our proposed PTDZ or the predicted direction of relative motion.

5.2. Nonactive Tectonic Elements

[36] To investigate the tectonic evolution of the Andrew Bain transform fault, we added a number of additional features to the tectonic chart. Shading depths shallower than 4000 m identifies the transform relay zone and the en echelon ridges and troughs south of this zone. In addition, the 4000 m contour to the north and a selected 5000 m contour to the south identify two long linear ridges lying north and south of the active plate boundary zone (A and B, Figure 5b). We found that the region of disturbed topography, existing between these two ridges and the elevated normal ocean floor to the west and east, has the shape of a flattened parallelogram (dashed line, Figure 5b). We have identified this region as the actual transform domain. In the direction of relative motion of Nubia/Antarctica, the domain has the same width as the separation between magnetic anomaly 6 on the Nubia/Antarctica plate boundary to the west [*Sclater et al.*, 1997] suggesting that the domain has existed only since Chron 6o (20 Ma).

6. Tectonic Models of the Transform Domain

[37] The existence of the transform relay zone and the occurrence of the inactive en echelon

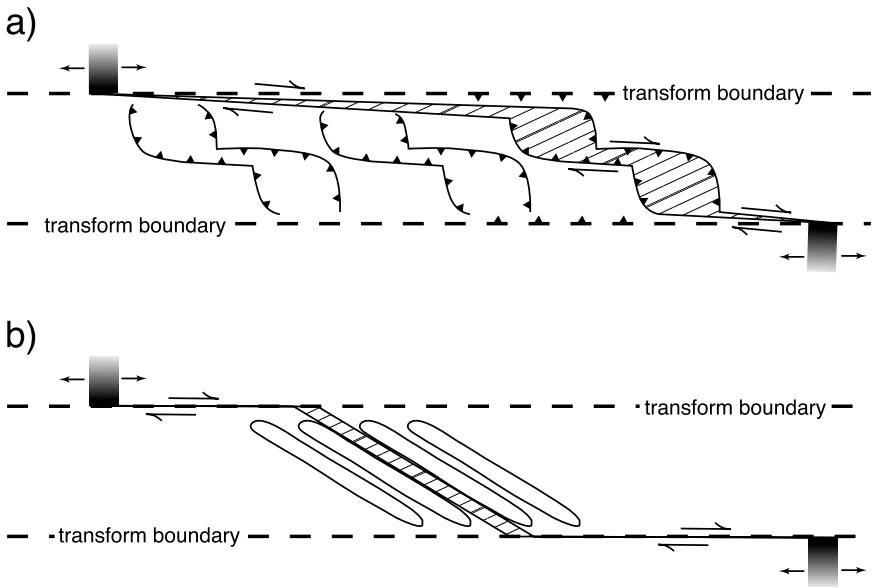

Figure 6. (a) Formation of arcuate pull-apart basins and a transform relay zone within a wide transform fault [after *Garfunkel*, 1986, Figure 6b]. Note the normal faulting on the transform boundaries, the earlier relay zones, and the asymmetric position of the currently active relay zone. (b) Formation of an oblique accretionary zone within a wide transform fault. Note the oblique, lenticular ridges formed either side of the accretionary zone (based on *Dick et al.* [2003, Figure 2]) which we have arbitrarily placed in a symmetric position within the transform domain. For both diagrams the width of the transform domain has been exaggerated and the stripes show the areas of active crustal accretion.

ridges and troughs to the south of this zone rule out most earlier explanations of the excessive width of transform domains. There is no evidence for a long-lived single intratransform spreading center or for a set of long-lived multiple offset transforms within the transform domain. In addition, we find no evidence for a series of obliquely stacked en echelon volcanic zones [*Taylor et al.*, 1994] that are the distinctive features of an extensional transform zone. Further, though the area of rough topography could be considered to have the shape of a lens, the model of *Ligi et al.* [2002] does not account for the either the transform relay zone or the en echelon ridges and troughs to the south of this zone. That model stresses a multiple fault component with two curved symmetric strike-slip faults accommodating the relative motion. These symmetric faults are not observed.

[38] Two plausible models remain. In the first, successive northward jumps of a transform relay zone created both the en echelon ridge-and-trough morphology to the south and the transform relay zone in the north (Figure 6a). In the second, a series of nontransform discontinuities [*Sauter et al.*, 2001]/oblique accretionary zones [*Dick et al.*, 2003] (Figure 6b) gave rise to the en echelon ridge-and-trough morphology with the presently active transform relay zone forming only in the last three to four million years.

6.1. Successive Transform Relay Zones

[39] In the successive transform relay zone concept, we assume that two overlapping pull-apart basins connected by an elongate transform-fault-dominated basin accommodate crustal extension within the transform domain during separation of Nubia from Antarctica. The formation of a succession of such relay basins (Figure 6a) gives rise to both the en echelon ridge-and-trough topography in the southeast and the active relay basins in the northeast of the transform domain (Figure 5b). This model has the advantage that it uses a concept that is active in the present to explain what has gone on in the past. However, the four southern en echelon ridges and troughs do not have the same morphology as the present-day relay basins. The troughs are neither as deep nor as broad. In addition, the ridges are lenticular in shape and lack the steep arcuate scarps of the highs either side of the relay basins. Finally, the ridges and intervening troughs are continuous along strike for significant distances (southeastern inset, Figure 4c). A relay zone consisting of several relay basins would generate discontinuous ridges and troughs with arcuate slopes of varying strikes.

6.2. Oblique Accretionary Zone

[40] An alternative suggestion is that the en echelon ridge and trough features in the south could have been created by a successive series of oblique accretionary zones (Figure 6b). *Dick et al.* [2003] have shown that such a zone has replaced a transform fault on the Southwest Indian Ridge between 11° and 14°E. This zone trends at about 30° to the spreading direction and is marked by an axial trough rarely more than a kilometer deep that extends for about 200 km. On the southern side of this trough between 13°E and 14°E lie two 50-km-long, 15-km-wide, and 1-km-high lenticular ridges [*Dick et al.*, 2003, Figure 2]. Like the main trough, each of these ridges makes an angle of 30° with the direction of spreading. They have no magnetic signature and are separated from each other by 20 km. Clearly these ridges have been created on the accretionary rift and then moved away from the axis by the emplacement of more material. Dredging and a weak magnetization suggest that these ridges are largely serpentenized peridotite. *Dick et al.* [2003] have argued that such oblique accretionary zones are a new class of plate boundary and a common feature on ultra-slow (<12 mm/yr) spreading ridges.

[41] The southern four ridges within the central en echelon ridge-and-trough sector of the Andrew Bain transform domain exhibit a similar morphology to the ridges on the SWIR between 11° and 14°E. Given that these four ridges trend at 30° to the direction of spreading, if they had been created by an oblique accretionary zone, they would have had at an effective spreading rate of 8 mm/yr [*Dick et al.*, 2003]. This is certainly slow enough to place them in the ultra-slow spreading rate category where oblique accretionary zones are common. We propose that such a zone created the en echelon ridge-and-trough morphology in the initial stages of development of the transform domain before transitioning into a relay zone at a later stage. We do not have an obvious explanation for this transition; though it could be related to a small change in the direction of the plate motion or changes in lithospheric strength with increasing proximity to the Marion Plume.

[42] We propose that throughout the entire tectonic development of the transform domain, a suite of overlapping and anastomising strike-slip faults connects the oblique accretionary zone/transfer relay zone to the southwestern spreading center and that a single strike-slip fault connects the relay zone to the northeastern spreading center. These assumptions and the proposition that the en echelon ridges and troughs represent a region of accretion permit us to construct a conceptual tectonic history of the Andrew Bain transform domain. We use reconstructions based on the published poles describing the motion of the Nubian plate with respect to the Antarctic plate as a framework for this conceptual history [*Lemaux et al.*, 2002; *Chu and Gordon*, 1999].

7. Tectonic History

[43] Currently a Chron 6o pole for the relative motion of Nubia/Antarctica does not exist making it impossible to provide a reliable base for a Chron 6o (20 Ma) reconstruction. However, we produced a speculative reconstruction by using the Chron 5o (11 Ma) pole of *Lemaux et al.* [2002] and extending the rate of spreading to 20 million years. By 20 Ma (Chron 6o) the entire area of the transform domain (bounded by the dashed line in Figure 5b) has disappeared and the two thin linear ridges to the north and south of the transform domain (A and B, Figure 7a) abut against each other. We speculate that prior to this time the Andrew Bain Fracture Zone consisted of two long transform faults of about equal length separated by a single orthogonal spreading center. This spreading center created the two narrow linear ridges. There is no clearly defined center of intrusion within the rest of the transform domain for older ocean floor. We speculate that the change from simple seafloor spreading to oblique accretion on the Andrew Bain occurred right after the break-up of the African plate into the Nubia and Somalia plates in the early Miocene [*Ebinger et al.*, 2000]. The change involved a small, approximately 5°, counterclockwise change in direction of motion. The western transform fault became a series of closely spaced transforms aligned parallel to the new direction of motion and the spreading center and long eastern transform fault became an oblique accretionary zone and a shorter more northerly trending transform (Figure 7a).

[44] Support for our speculation regarding a change in direction of motion of the Nubia/Antarctica plate boundary comes from the indication of a 5° to 10° counterclockwise shift in the trace of the Du Toit Fracture Zone around the projected position of Chron 6o (20 Ma) north of the SWIR (~51°S, 27°30′E, Figure 1). Our closely spaced western transform faults on the Andrew Bain are similar to those identified by *Searle* [1983] within the Quebrada Fracture zone or the more complex

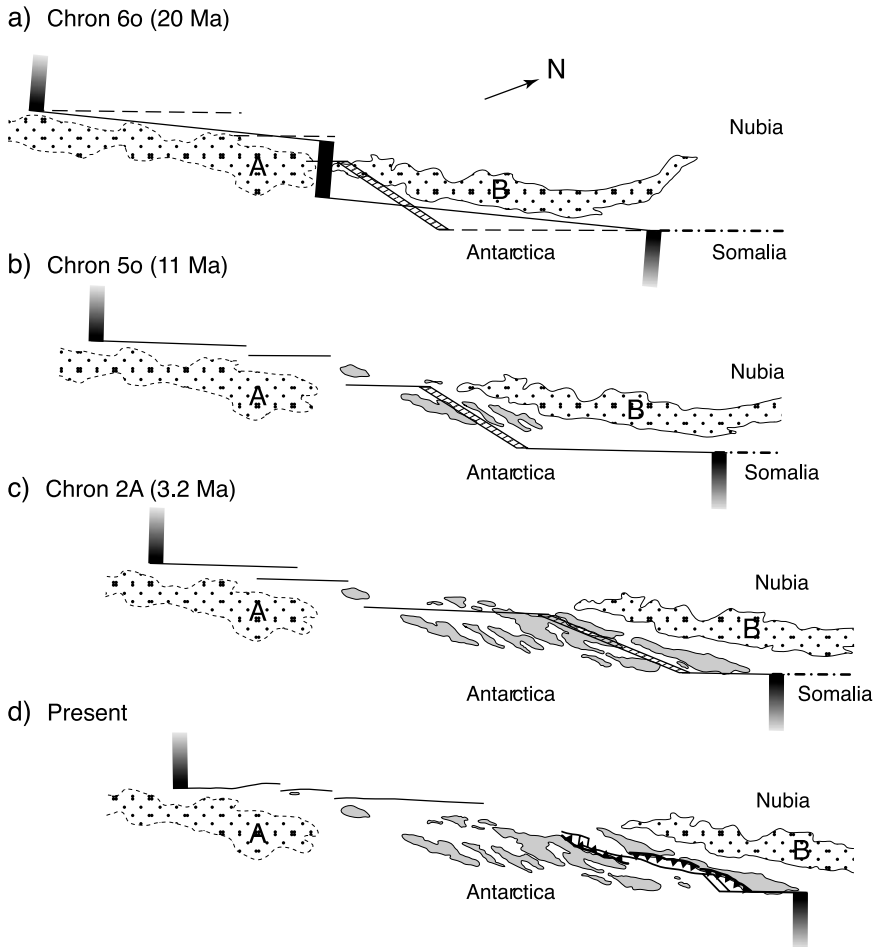

Figure 7. A tectonic history of the Andrew Bain transform domain from Chron 6o (20 Ma) to the present. Filled in rectangles, spreading centers at the southwestern and northeastern ends of the transform fault; heavy lines, transform faults; cross-hatched lines, position of the oblique accretionary zone; stippled areas, linear ridges A and B south and north of the transform domain; light gray areas, areas shallower than 4000 m within the domain; dash dot line, Nubia/Somalia plate boundary. (a) Chron 6o (20 Ma) reconstruction. Dashed lines show new position of the transform faults after the change in spreading direction. (b) Chron 5o (11 Ma) reconstruction. (c) Chron 2A (3.2 Ma) reconstruction. (d) Present. The concave hatched lines represent the active faults defining the extent of the relay basins. For discussion, see text.

features recognized by *Tucholke and Schouten* [1988] on 84–90 Ma crust of the Kane Fracture Zone either side of the mid-Atlantic ridge.

[45] As a basis for the Chron 5o (11 Ma) reconstruction, we rotated the northern ridge (B, Figure 5b) toward the Antarctic plate [*Lemaux et al.*, 2002]. In addition, we removed an area, representing the ocean floor created between Chron 5o (11 Ma) and the present, from the northern section of the domain. Only the southern en echelon ridge and trough topography remained. The central trough is both wider and deeper than those on either side (Figure 4c and inset). We placed the oblique accretionary zone within this trough. At 11 Ma, the plate boundary consisted of a suite of en echelon strike-slip faults in the southwest connected by an oblique accretionary zone to a single transform fault in the northeast (Figure 7b). Two elongate ridges lay north and south of the oblique accretionary zone (A and B, Figure 7b) and formed the limits of the transform domain. A linear ridge lying roughly parallel to the direction of relative motion of Nubia/Antarctica has started to develop between the two transform faults lying just west of the oblique accretionary zone.

[46] For the Chron 2A (3.2 Ma) reconstruction, we rotated the northern ridge (B, Figure 7c) toward the Antarctic plate about pole of *Chu and Gordon* [1999]. This rotation closed the transform relay basins. We placed the oblique accretionary zone

within the center of the elongate ridges and troughs trending at 20° to the direction of spreading. We assume that the different trends of the en echelon ridges and troughs south of the relay zone mark different oblique accretionary episodes. The plate boundary consisted of a suite of overlapping strike-slip faults in the southwest connected by an oblique accretionary zone to a shorter strike-slip fault in the northeast (Figure 7c). The two elongate ridges now form the northern and southern limits of a much wider transform domain (A and B, Figure 7c). A pronounced ridge (only the 4000 m contour appears in Figure 7c) has developed between the two strike-slip faults that lie just west of the oblique accretionary zone. As a result of the accretionary zone jumping to the north, the overlapping southwestern strike-slip faults have lengthened and the single northeastern strike-slip fault has shortened.

[47] We suggest that, close to Chron 2A (3.2 Ma), the oblique accretionary zone terminated with the zone of extension jumping northward to become a series of overlapping transform relay basins (Figure 7d). Just west of the oblique accretionary zone, motion terminated on the strike-slip fault. The southwestern section of the Andrew Bain became a suite of closely spaced strike-slip faults that lay entirely within the deep valley close to the western edge of the transform domain (Figure 7d). Since 20 Ma, these strike-slip faults have lengthened by 75 km and the single northeastern transform fault has become shorter by about 275 km. The formation of the relay zone accounts for the difference between these two figures. In combination theses changes and the formation of a transform relay zone have created the present 750-km-long transform boundary between the Nubian and Antarctic plates (Figure 7d).

[48] We have assumed that each oblique accretionary zone episode involved symmetrical accretion. This does not have to be the case. Accretion could have occurred simultaneously at a number of sites creating a broad zone of extension. Conceptually, our tectonic history would work equally well if the accretion occurred within a series of transform relay zones that jumped successively northward. We prefer the oblique accretionary zone model because it provides a better morphological explanation of the region of en echelon ridges and troughs lying south of the presently active relay zone.

[49] Our speculative tectonic history for the Andrew Bain transform domain makes two predictions. First, a normal orthogonal mid-ocean spreading center created the ridges north and south of the domain (A and B, Figure 5b). Thus identifiable magnetic anomalies should be observed over these features. In fact, some small 200 nT anomalies have been reported over the northern portion of Ridge B but they have not been identified [*Sclater et al.*, 1997]. Second, an oblique amagmatic accretionary zone gave rise to the lineated en echelon ridges and troughs within the domain. By analogy with the results of *Dick et al.* [2003] for the SWIR between 11° and 14°E, dredging of these ridges should yield dominantly ultramafic rocks.

8. Conclusions

[50] We have shown that, between 3.2 Ma and the present, the Nubia/Somalia plate boundary intersects the SWIR east of the Prince Edward transform fault. Combining this information with the 11 Ma position of this plate boundary [*Lemaux et al.*, 2002], we argue that the Andrew Bain transform fault has lain on the Nubia/Antarctica plate boundary probably for the past 20 million years. Even though part of this boundary, the overall trend of the transform domain lies 10 degrees clockwise of the predicted direction of motion of Nubia/Antarctica.

[51] The Andrew Bain transform fault consists of a long, deep southwestern valley connected via a series of overlapping basins to a much shorter, narrower, and shallower northeastern valley. To the south of these basins lies a suite of inactive en echelon ridges and valleys that make an angle of between 10° and 30° with the predicted direction of spreading. The region of complex topography lying between the southwestern and northeastern spreading centers fits within a flattened parallelogram that has existed probably only for the past 20 million years.

[52] We interpret the overlapping basins as two pull-apart features connected by a strike-slip dominated basin that have created a relay zone similar to those observed on continental transforms. This transform relay zone connects three long closely spaced en echelon strike-slip faults in the southwest to a single short strike-slip fault in the northeast. This zone accounts for most of the difference between the observed trend of the transform boundary and the direction predicted by the relative motion of Nubia/Antarctica. We believe we can trace the PTDZ from the northern RTI to the northern relay basin and then follow its trace through the rest of the relay zone.

[53] The present plate boundary configuration that we propose is different than that predicted by thermal modeling of long, slow-slip transform boundaries and geologic observations. *Ligi et al.* [2002] propose that mega-transforms such as the Romanche in the equatorial Atlantic accommodate relative motion along two curved symmetric strike-slip zones that extend the entire length of the transform domain. When examined in detail, the Andrew Bain transform domain has neither an oval shaped region of rough topography, nor a single long and continuous fault that defines the active plate boundary zone. We speculate that these differences occur for a number of reasons. First, the Andrew Bain transform fault has never been a single, long strike-slip fault. We suggest that it has always consisted of a number of strike-slip faults, separated by one or more zones of crustal accretion, and that the age offset has never been large enough to permit the formation of lens of anomalously thick and cold lithosphere around the center of the transform. Second, we argue that the Andrew Bain transform fault has been a transtensive feature, whereas the Romanche transform fault has been alternatively transtensive and transpressive [*Bonatti et al.*, 1994]. Finally, the northern sector of the Andrew Bain transform fault appears to mark the western limit of Marion plume influence on the SWIR [*Georgen et al.*, 2002]. No such feature lies close to the Romanche transform fault. The increased temperatures and magma supply associated with this plume appear to have a significant impact on the rheological response of the lithosphere in the northern sector of the Andrew Bain transform fault. For example, the Marion plume could create a warmer mantle in the north so that the northern part of the transform behave more like a slow-to-medium slip ridge whereas the southern end is colder and hence behaves more like an ultra-slow ridge. If correct this suggests that the changes seen in the spreading regime near plumes (e.g., Reykjanes Ridge) may have a counterpart in the slip regime.

[54] Prior to 20 Ma, we speculate that the Andrew Bain transform fault consisted of two, almost equally long, transform faults offset by a short, orthogonal intratransform spreading center. At 20 Ma spreading along the intratransform segment became highly oblique, most likely due to a change in relative plate motion. This reduced the effective spreading rate along this segment to less than 8 mm/yr resulting in oblique amagmatic accretion. We suggest that between 20 and 3.2 Ma the accretionary zone jumped successively northward and created the oblique en echelon ridges and valleys, effectively lengthening the southwestern and almost eliminating the northeastern transform fault. During the final northward jump at 3.2 Ma the style of accretion changed to that of a transform relay zone.

Acknowledgments

[55] This work was supported by grants NSFOCE03-29565, NSFOCE97-96254, and NSFOCE93-14324 to John Sclater, Nancy Grindlay, and John Madsen, respectively. We are grateful to Nancy Bowers for first suggesting that we apply models of continental deformation in the interpretation of the oceanic data. Peter Shearer provided the various seismological compilations for our use, and Gabe Laski explained the intricacies of CMT solutions to us. We constructed the charts using the GMT mapping tool of *Wessel and Smith* [1995]. Roger Searle, Marco Ligi, Daniel Sauter, and Robert Fisher provided constructive critiques of the evolving manuscript.

References

Aydin, A., and A. Nur (1982), Evolution of pull-apart basins and their scale independence, *Tectonics*, *1*(1), 91–105.

Bergh, H. W. (1977), Mesozoic sea-floor off Dronning-Maud-Land, Antarctica, *Nature*, *269*(5630), 686–687.

Bonatti, E., M. Ligi, L. Gasperini, A. Peyve, Y. Raznitzin, and Y. J. Chen (1994), Transform migration and vertical tectonics at the Romanche Fracture Zone, equatorial Atlantic, *J. Geophys. Res.*, *99*(B11), 21,779–21,802.

Cande, S. C., J. L. LaBrecque, and W. F. Haxby (1988), Plate kinematics of the South Atlantic: Chron C34 to present, *J. Geophys. Res.*, *93*(B11), 13,479–13,492.

Chu, D., and R. G. Gordon (1999), Evidence for motion between Nubia and Somalia along the Southwest Indian Ridge, *Nature*, *398*(6722), 64–66.

DeMets, C., R. G. Gordon, D. F. Argus, and S. Stein (1990), Current plate motions, *Geophys. J. Int.*, *101*(2), 425–478.

Dick, H. J. B., J. Lin, and H. Schouten (2003), An ultraslow-spreading class of ocean ridge, *Nature*, *426*(6965), 405–412.

Dziewonski, A. M., et al. (1983–1999), Centroid-moment tensor solutions 1977–1998, *Phys. Earth Planet.*, 33–115.

Dziewonski, A. M., et al. (2000–2003), Centroid-moment tensor solutions 1999–2000, *Phys. Earth Planet. Inter.*, 116–135.

Ebinger, C. J., T. Yemane, D. J. Harding, S. Tesfaye, S. Kelley, and D. C. Rex (2000), Rift deflection, migration, and propagation: Linkage of the Ethiopian and Eastern rifts, Africa, *Geol. Soc. Am. Bull.*, *112*(2), 163–176.

Ekstrom, G., et al. (2003), Global seismicity of 2001: Centroid-moment tensor solutions for 961 earthquakes, *Phys. Earth Planet. Inter.*, *136*, 165–185.

Engdahl, E. R., R. van der Hilst, and R. Buland (1998), Global teleseismic earthquake relocation with improved travel time procedures for depth determination, *Bull. Seismol. Soc. Am.*, *88*(3), 722–743.

Fisher, R. L., and A. M. Goodwillie (1997), The physiography of the Southwest Indian Ridge, *Mar. Geophys. Res.*, *19*(6), 451–455.

Fisher, R. L., M. Z. Jantsch, and R. L. Comer (1982), GEBCO Panel 5.09, IHO/IOC/CHS, in *GEBCO—General Bathymetric Chart of the Oceans*, 5th ed., Int. Hydrogr. Organ.,

Intergovt. Oceanic Comm., Can. Hydrogr. Ser., Ottawa, Ontario, Canada.
Fisher, R. L., H. J. B. Dick, J. H. Natland, and P. S. Meyer (1986), Mafic/ultramafic suites of the slowly spreading Southwest Indian Ridge: PROTEA exploration of the Antarctic plate boundary, *Ofioliti*, *11*, 147–178.
Fox, P. J., and D. G. Gallo (1984), A tectonic model for ridge-transform-ridge plate boundaries: Implications for the structure of oceanic lithosphere, *Tectonophysics*, *104*(3–4), 205–242.
Garfunkel, Z. (1986), Review of oceanic transform activity and development, *J. Geol. Soc. London*, *143*, 775–784.
Georgen, J. E., J. Lin, and H. J. B. Dick (2002), Evidence from gravity anomalies for interactions of the Marion and Bouvet hotspots with the Southwest Indian Ridge: Effects of transform offsets, *Earth Planet. Sci. Lett.*, *187*(3–4), 283–300.
Goodwillie, A. M. (1996), Producing gridded databases directly from contour maps, *SIO Ref. Ser., 96-17*, 33 pp., Scripps Inst. of Oceanogr., Univ. of Calif., San Diego, La Jolla.
Grindlay, N. R., J. A. Madsen, C. Rommevaux-Jestin, J. Sclater, and S. Murphy (1996), Southwest Indian Ridge 15°E–35°E: A geophysical investigation of an ultra-slow spreading mid-ocean ridge system, *InterRidge News*, *5*, 7–12.
Grindlay, N. R., J. A. Madsen, C. Rommevaux-Jestin, and J. Sclater (1998), A different pattern of ridge segmentation and mantle Bouger gravity anomalies along the ultra-slow Southwest Indian Ridge (15°30′E to 25°E), *Earth Planet. Sci. Lett.*, *161*(1–4), 243–253.
LaBrecque, J. L., and D. E. Hayes (1979), Seafloor spreading history of the Aguhlas Basin, *Earth Planet. Sci. Lett.*, *45*(2), 411–428.
Lemaux, J., R. G. Gordon, and J.-Y. Royer (2002), Location of the Nubia-Somalia boundary along the Southwest Indian Ridge, *Geology*, *30*(4), 339–342.
Ligi, M., E. Bonatti, L. Gasperini, and A. N. B. Poliakov (2002), Oceanic broad multifault transform plate boundaries, *Geology*, *30*(1), 1–14.
Lonsdale, P. (1994), Structural geomorphology of the Eltanin fault system and adjacent transform faults of the Pacific-Antarctic plate boundary, *Mar. Geophys. Res.*, *16*(2), 105–143.
McKenzie, D. P., and R. L. Parker (1967), The North Pacific: An example of tectonics on a sphere, *Nature*, *224*, 125–133.
Menard, H. W., and T. Atwater (1969), Origin of fracture zone topography, *Nature*, *222*, 470–473.
Morgan, W. J. (1968), Rises, trenches, great faults and crustal blocks, *J. Geophys. Res.*, *73*, 1959–1982.
Nettles, M., and G. Ekstrom (1998), Faulting mechanism of anomalous earthquakes near Bardarbunga Volcano, Iceland, *J. Geophys. Res.*, *103*(B8), 17,973–17,983.
Okal, E. A., and S. Stein (1987), The 1942 Southwest Indian Ridge earthquake: Largest ever recorded on an oceanic transform, *Geophys. Res. Lett.*, *14*(2), 147–150.
Pockalny, R. A., P. J. Fox, D. J. Fornari, K. C. Macdonald, and M. R. Perfit (1997), Tectonic reconstruction of the Clipperton and Siqueiros Fracture Zones: Evidence and consequences of plate motion change for the last 3 Myr, *J. Geophys. Res.*, *102*(B2), 3167–3187.
Royer, J.-Y., P. Patriat, H. W. Bergh, and C. R. Scotese (1988), Evolution of the Southwest Indian Ridge from the Late Cretaceous (Anomaly 34) to the Middle Eocene (Anomaly 20), *Tectonophysics*, *155*(1–4), 235–260.
Sandwell, D. T., and W. H. F. Smith (1997), Marine gravity anomaly from Geosat and ERS 1 satellite altimetry, *J. Geophys. Res.*, *102*(B5), 10,039–10,054.
Sauter, D., P. Patriat, C. Rommevaux-Jestin, M. Cannat, and A. Briais (2001), The Southwest Indian Ridge between 49°15E and 57°E: Focused accretion and magma redistribution, *Earth Planet. Sci. Lett.*, *192*(3), 303–317.
Sclater, J. G., M. Munschy, R. L. Fisher, P. A. Weatherall, S. C. Cande, P. Patriat, H. Bergh, and R. Schlich (1997), Geophysical synthesis of the Indian/Southern Oceans; Part 1, The Southwest Indian Ocean, *SIO Ref. Ser.*, *97-06*, 45 pp., Scripps Inst. of Oceanogr., Univ. of Calif., San Diego, La Jolla.
Searle, R. C. (1983), Multiple, closely spaced transform faults in fast-slipping fracture zones, *Geology*, *11*(10), 607–610.
Searle, R. C., M. V. Thomas, and E. J. W. Jones (1994), Morphology and tectonics of the Romanche Transform and its environs, *Mar. Geophys. Res.*, *16*(6), 427–453.
Segoufin, J. (1978), Anomalies magnetiques dans la basin de Mozambique, *C. R. Acad. Sci. Paris, Ser. D.*, *287*, 102–109.
Shaw, P. R., and S. C. Cande (1990), High-resolution inversion for South Atlantic plate kinematics using joint altimetry and magnetic anomaly data, *J. Geophys. Res.*, *95*(B3), 2625–2644.
Shearer, P. M. (2001), Improving global seismic event locations using source-receiver reciprocity, *Bull. Seismol. Soc. Am.*, *91*(3), 594–603.
Simpson, E. S. W., J. G. Sclater, B. Parsons, I. O. Norton, and L. Meinke (1979), Mesozoic magnetic lineations in the Mozambique Basin, *Earth Planet. Sci. Lett.*, *43*(2), 260–264.
Taylor, B., K. Cook, and J. Sinton (1994), Extensional transform zones and oblique spreading centers, *J. Geophys. Res.*, *99*(B10), 19,707–19,718.
Tucholke, B. E., and H. Schouten (1988), Kane fracture zone, *Mar. Geophys. Res.*, *10*(1), 1–39.
Wald, D. J., and T. C. Wallace (1986), A seismically active section of the Southwest Indian Ridge, *Geophys. Res. Lett.*, *13*(10), 1003–1006.
Wessel, P., and W. H. F. Smith (1995), New version of the Generic Mapping Tools released, *Eos Trans. AGU*, *76*, 329.
Wilson, J. T. (1965), A new class of fault and their bearing on continental drift, *Nature*, *207*, 343–347.